
# The SOLASE Laser Fusion Reactor Design and Its Technological Implications

R.W. Conn, S.I. Abdel-Khalik, G.A. Moses, G.W. Cooper, J.E. Howard, E.M. Larsen, I.N. Sviatoslavsky, and W.G. Wolfer

October 1977

UWFDM-229

Presented at IAEA Conf. and Workshop on Fusion Reactor Design, Madison, October 1977, IAEA-TC-145/17, 269-298 (1978).

FUSION TECHNOLOGY INSTITUTE

UNIVERSITY OF WISCONSIN

MADISON WISCONSIN

# The SOLASE Laser Fusion Reactor Design and Its Technological Implications

R.W. Conn, S.I. Abdel-Khalik, G.A. Moses, G.W. Cooper, J.E. Howard, E.M. Larsen, I.N. Sviatoslavsky, and W.G. Wolfer

Fusion Technology Institute
University of Wisconsin
1500 Engineering Drive
Madison, WI 53706

http://fti.neep.wisc.edu

October 1977

UWFDM-229

Presented at IAEA Conf. and Workshop on Fusion Reactor Design, Madison, October 1977, IAEA-TC-145/17, 269-298 (1978).

"LEGAL NOTICE"

"This work was prepared by the University of Wisconsin as an account of work sponsored by the Electric Power Research Institute, Inc. ("EPRI"). Neither EPRI, members of EPRI, the University of Wisconsin, nor any person acting on behalf of either:

"a. Makes any warranty or representation, express or implied, with respect to the accuracy, completeness, or usefulness of the information contained in this report, or that the use of any information, apparatus, method, or process disclosed in this report may not infringe privately owned rights; or

"b. Assumes any liabilities with respect to the use of, or for damages resulting from the use of, any information, apparatus, method or process disclosed in this report."

# The SOLASE Laser Fusion Reactor Design and Its Technological Implications

R. W. Conn
S. I. Abdel-Khalik
G. A. Moses
G. W. Cooper
J. E. Howard
E. M. Larsen
I. N. Sviatoslavsky
W. G. Wolfer

Fusion Research Program
Nuclear Engineering Department
University of Wisconsin
Madison, Wisconsin 53706

UWFDM-229

October 1977

Paper presented at the IAEA Technical Meeting and Workshop on Fusion Reactor Design, Madison, Wisconsin (October 10-21, 1977).
**Published in Fusion Reactor Design Concepts, IAEA, Vienna (1978).**

## Abstract

A conceptual laser fusion reactor has been designed to elucidate the technological problems posed by inertial confinement fusion reactors. A general description of the reactor concept is presented and the major technological implications of the study are summarized. Results from experiments over the next five to seven years taken together with the findings of studies such as SOLASE will provide the basis for determining if an ambitious engineering-oriented program aimed at reactor development is warranted.

## I. Introduction

Research on inertial confinement fusion has expanded dramatically in recent years and experimental results on compression and neutron yields from laser[1-4] and electron beam[5-6] illuminated targets are measures of the rapid progress. The theory that suggested the possibility of achieving high gains by illuminating small spherical deuterium-tritium targets[7-8] has also grown rapidly. The progress is such that several energy break-even experiments are planned for the not too distant future. Given both this progress and the level of research effort, it is worthwhile at this time to determine the requirements for inertial confinement fusion reactors and to examine the technological problems such systems might pose. In turn, such work can provide the basis for more substantial efforts on the most important reactor technology problems.

Laser initiated thermonuclear fusion is presently the most widely studied inertial confinement area. To examine laser fusion technology problems, we have developed a conceptual laser fusion power reactor for electric power production and called the system SOLASE.[a] This research should help lay a foundation to make a more realistic assessment of the ultimate potential of laser fusion reactors. We describe in this paper the major features of the SOLASE design and summarize the key conclusions and technological implications of the study. Greater detail on all topics can be found in an extensive report.[9]

---

[a] SOLASE, as in "their solase in dorckaness, and splattering together joyously the plaps of their tappyhands as, with one cry of genuine distress, so prettly prattly pollyogue, they viewed him, the just one, their darling, away."
J. Joyce, Finnegans Wake, The Viking Press, New York (1939), p. 470.

## II. General Description of SOLASE

The main parameters characterizing the SOLASE conceptual laser fusion power reactor are listed on Tables 1 and 2. A top view of the entire SOLASE power plant is given in Fig. 1 and a more detailed view of the reactor cavity is shown in Fig. 2. The system has a pellet gain of 150 and the laser energy on target is 1 MJ. The cavity is spherical with a radius of 6 m and the average neutron wall loading is 5 $MW/m^2$. The blanket design is based on the use of lithium oxide ($Li_2O$) ceramic microspheres (50-100 μm radii) flowing under gravity through a structure made from chopped fiber graphite composite. The temperature of the graphite and lithium oxide can be effectively decoupled in this design, an important feature in avoiding excessive radiation damage. There are twelve final mirrors of diamond turned Cu on Al cooled with water which illuminate the target from two sides. The cavity first wall and last mirror are protected from charged particle pellet debris by a low density (0.5 torr at 300°C) neon or xenon buffer gas. Neon was chosen initially because it has the highest breakdown threshold but xenon is an alternate and perhaps preferable choice because it can simultaneously stop the X-rays as well as ions. Only experiments will allow a clear choice. It appears gas breakdown can occur but its effect may be minimal for large reactor size pellets where the target radius can exceed 2 mm.

The laser system is designed as generically as possible but is modeled after the $CO_2$ laser where specificity is required. This is not necessarily ideal from a target physics interaction point of view and this choice

is not a specific endorsement of $CO_2$. Rather it is a recognition that the $CO_2$ laser has many of the characteristics of the desirable laser for laser fusion. With multipassing the estimated overall efficiency is 6.7% and the maximum final amplifier energy is 45.8 kJ. There are 6 final amplifiers and the 24 beams are subsequently recombined to 12 final beams.

The system power cycle outlined in Fig. 3 shows that the $Li_2O$ transports heat directly to steam generators which then drive turbines producing 1334 $MW_e$ gross. The laser recirculating power requirement is 300 $MW_e$ and other internal plant power requirements lead to a net plant electrical output of 1000 $MW_e$ and a net thermal efficiency of 30%. The level of 1000 $MW_e$ net output is chosen as representation of a full scale unit. It does not imply smaller units more appropriate during a reactor development stage are less attractive or impossible to design. The large recirculating laser power fraction appears typical of laser fusion systems unless a gain much larger than 150 or a laser efficiency much greater than 5 to 10% can be achieved. The following analysis demonstrates this point.

The pellet gain is defined as the ratio of thermonuclear energy produced (Y) to the laser energy incident on the pellet ($E_L$). For breakeven the gain must equal unity but for power plant applications the necessary gain is determined by the laser efficiency and plant thermal efficiency. The relation between these quantities is given by the expression

$$G = \left[\frac{1}{\eta_L\,(\eta_{th}-\eta_p)}\right] - 1 \qquad (1)$$

where $\eta_L$ is the laser efficiency, $\eta_{th}$ is the gross plant thermal efficiency, and $\eta_p$ is the net plant thermal efficiency.

If we make the reasonable assumption that (1) the gross thermal efficiency is about 40%, (2) that the net plant efficiency must be at least 30% from economic and environmental considerations, and (3) that the laser efficiency is about 10%, then the pellet gain must be 100. For a laser efficiency of 5% the pellet gain must be 200. Therefore realistic gross and net plant efficiencies and optimistic values of laser efficiency indicate that a pellet gain of 100 to 200 is necessary for reactor applications. The SOLASE design requires a pellet gain of 150 because the laser design with multi-passed amplifiers has an efficiency of 6.7%. For a 1 MJ laser this gain implies a pellet yield of 150 MJ.

## III. Last Mirror and Laser Design

The last mirror is diamond turned copper on an aluminum backing and structure with the shape of an off-axis paraboloid. It is found that neutron induced damage is not a serious problem. Neutron damage of the Cu on Al substrate mirror at 15 m from pellets with a 150 MJ yield ignited at a rate of 20 Hz is low, about $10^{-7}$ dpa/sec, and the neutron heating is less than 10 $W/cm^3$. This provides little incentive to move the mirror farther than 15 meters from the target. In addition pointing errors grow increasingly greater as the mirrors are moved far from the target. In the limit of very large distances (50 to 100 meters) the size of the primary containment building becomes an important issue if the last mirror must still reside within it. The neutronics analysis of course does not demand that mirrors be placed at these distances.

Surface damage to the mirror by X-rays and pellet debris is a much more significant problem. Large quantities of pellet debris on the mirror surface cannot be tolerated because physical and more importantly chemical reactions at the mirror surface will degrade its optical quality. This is an important reason to choose chemically compatible pellet and mirror materials. One method to protect the mirror is essentially the same as the gas protection scheme for the cavity first wall. Pellet debris is stopped by a flowing gas such as xenon or neon in front of the mirror surface as shown schematically in Fig. 4. All six laser beam lines pass through a suppression chamber on the outside. As the pellet debris flows out through the blanket beam ports it expands in this chamber. This reduces the shock strength while the actively-cooled walls of the chamber cool the debris before it reaches the vacuum pumps. The walls of the beam lines from the chamber to the last mirror are also actively cooled and neon or xenon gas flows at low pressure from near the mirror surface toward the suppression chamber. Hot debris diffusing into this beam line is cooled by convection until the diffusion rate of the debris is sufficiently low that the flowing gas will convect it away from the mirror surface. This method has been used on a small scale to protect optical windows from hot expanding plasmas in laser-plasma experiments and appears suitable for laser fusion reactor applications.

The use of 12 final laser beams to illuminate the target from two sides does not provide uniform target illumination. In SOLASE for example at least 20 beams would be required for uniform illumination if 10% of the

allowed solid angle can be devoted to beams. The diameter of the last optical element with f/2.74 located 15 m from the target would be 5.5 m, clearly very large. One could locate the mirrors closer to the target to reduce their size but this in turn increases the difficulty of protecting the mirrors and complicates cavity design by reducing accessibility. If future pellet designs require more uniform illumination than provided in SOLASE, laser fusion reactors will be much more difficult to realize.

Prevention of damage to the various optical components in the beam train will limit the damage energy density threshold for nanosecond pulses to about 1 to 10 $J/cm^2$. For the generic laser design in SOLASE, a value of 3 $J/cm^2$ has been chosen. Combining this limiting energy density value with the total laser energy output required for target performance determines the minimum total aperture of the laser.

The number of final amplifiers chosen depends on the largest size of a single amplifier and the number of beams required to illuminate the target. For SOLASE the total energy output requirement for each amplifier is reduced by multipassing the last two amplifiers and combining the beams in pairs. This limits the output of each amplifier to less than 50 KJ per pass (a realistic value for the average laser system) and simultaneously increases the laser efficiency at short pulse lengths. For $CO_2$ the lower single pass efficiency is due to the fact that the normally advantageous collisional processes have insufficient time to contribute to the pumping process. Only that energy stored directly in the upper laser level contributes to the energy output for a nanosecond pulse. The maximum

laser efficiency is thus limited to a few percent. The efficiency could be improved by utilizing a multi-passing technique which allows time for the collisional repopulation of the upper laser level. In the SOLASE design, there are six final amplifiers and four beams are successively from each amplifier. The aperture per beam is about 1.527 $m^2$ and the total input energy required to drive an amplifier is 4720 J per amplifier per pass. Since the total energy output per amplifier per pass is 45.8 kJ, the input energy will comprise over 10% of the total output energy. It is therefore desirable to multi-pass the next-to-last stage of the amplifier chain to improve its efficiency as well as that of the last stage. Assuming the same basic parameters as for the final amplifier, the next to last amplifier will require an aperture of 0.1573 $m^2$ and an input driving energy of 486 J.

For successful operation of a four beam multi-pass amplifier, the passage of each beam through the amplifier must be separated by sufficient time to allow the upper laser level to repopulate. At 1800 torr this time is approximately 0.1 μs. After passing through the amplifiers, each beam must be delayed the appropriate amount in order that all beams reach the target simultaneously. The delay lines are indicated by the dashed lines in the laser building shown on Fig. 1.

The final amplifier in the SOLASE laser design shown in Fig. 5 is 2.5 m in length, and has a small signal gain of 0.04 $cm^{-1}$. It is a segmented annulus and the inner and outer diameters of the pumping volume are 298 and 372 cm, respectively. There are 24 segments

(34 cm x 37 cm in cross section) spaced 5 cm apart at the inner radius. The laser beam itself is annular with an inner diameter of 13 cm and an outer diameter of 357 cm. The distance between the input and output mirrors is 100 m. The angle the beams make with respect to the center axis of the amplifier is 60 mrad. With these values of the parameters, 59% of the volume can be extracted per pass. This corresponds to an aperture area of 1.775 $m^2$. Since only 1.527 $m^2$ is required for a uniform plane wave of 3 $J/cm^2$ to yield the required output, this design has a geometric utilization factor of 86%.

## IV. Reactor Cavity and Blanket Design

The reactor cavity in the SOLASE design is filled with neon or xenon gas at less than 1 torr pressure. This is sufficient to protect the front wall from the ions and soft X-rays produced by the microexplosion. The energy deposited in the gas is radiated to the front wall over a relatively long time period (>1 ms) so that surface heating and thermal ablation of the wall become insignificant. Since a complete pellet design is unavailable now, parametric studies have been carried out using the PHD-IV pellet burn code[10] to provide input information on the possible variability of the X-ray and particle debris spectra.

The range in neon of the different particles found in the pellet at energies that appear to be a maximum for the given particle are summarized in Table 3. The calculations are based on Lindhard stopping theory[11] which is most accurate for the heavy ions. Since only enough gas is placed in the chamber to prevent particles from hitting the wall, these particles deposit their energy in the gas over a large volume. As such, strong shock theory is not applicable and we have developed a Lax-Wendroff fluid

dynamics code for the problem.[12] Shocks are observed to develop but they are weak because of the rather weak initial condition. The peak values for the kinetic energy fraction and the total momentum in the shock are about half those given by strong shock theory. The peak pressure at the wall is about 90 torr and is spread in time over about $5 \times 10^{-4}$ seconds. The momentum transferred to the wall, obtained by integrating the pressure profile over time, is about $2 \times 10^{8}$ g cm/sec.

Hard X-rays deposit their energy directly in the front graphite wall of the blanket but produce a relatively small surface temperature rise because they have a sufficiently long range. Soft X-rays are stopped in the gas when xenon is used. The temperature rise in the first wall is given in Fig. 6 as a function of the black body temperature used to characterize the X-ray spectrum. Results for two different fill gases, neon and xenon, at two different fill pressures are given. For this case, the energy in X-rays is 15 MJ (10% of the yield). $\Delta T$ will scale linearly with the energy in X-rays for a given black body temperature.

The pulsed surface heat flux radiating from the gas is rectified in the front wall of the blanket and directly convected and radiated to the flowing lithium oxide. The combined heat transfer coefficient is low (~0.2 $W/cm^2$-°C) so that the front wall temperature is significantly higher than the temperature of the $Li_2O$ stream. As shown in Fig. 7, the lithium oxide particles enter the blanket at 400°C and leave at 600°C, except for the outermost zone where the exit temperature is 850°C. (This hot stream contains 2% of the total flow rate and is used for tritium extraction). The back surface of the front wall will operate at about 1400°C and the front surface temperature reaches approximately 1800°C after each

microexplosion. These temperatures are sufficiently high that excessive swelling of the graphite should not be a problem. At these temperatures the vapor pressure of carbon remains low so that thermal ablation of the graphite is insignificant.

The blanket is constructed primarily of graphite. Either nuclear grade graphite or chopped-fiber type graphite composite can be used. Lithium oxide particles, 100-200 μm in diameter, flow under gravity through the blanket and serve the dual purpose of tritium breeding and heat transport. The spherical cavity is divided along longitudes into sixteen blanket segments each with a honeycomb-type construction (Figs. 2 and 7). The tangential spacers parallel to the front wall allow the velocity distribution of the $Li_2O$ particles to be tailored to match the radial heat deposition curve. The radial supports provide structural rigidity and allow impulse loadings on the front wall to be transmitted to the support structure behind the blanket. This design eliminates the need for metallic first walls and liners since the front wall of the blanket can readily accommodate the microexplosion both thermally and mechanically.

The tangential spacers parallel to the front wall will operate at nearly 650°C since the amount of heat generated within them is low. At 650°C volume changes in the graphite upon irradiation are also low. This means that the graphite temperature in the blanket is either above or below the temperature region (~850-1150°C) where excessive swelling limits graphite performance. The temperature gradient between the front wall and the first tangential spacer is accommodated by ceramic radial supports. The estimated lifetime of the blanket structure at 5 $MW/m^2$

wall loading is approximately 1 year (~30 dpa). Given the relative ease with which blanket replacement can be accomplished here, (based on accessibility and the fact that graphite blanket segments will simply be replaced, not refurbished )this lifetime should be adequate.

A special feature of the $Li_2O$/graphite blanket is the very low level of induced radioactivity and the adequate breeding ratio. Detailed neutronic calculations give a breeding ratio of 1.33. A calculation of the blanket radioactivity as a function of time after shutdown shows that the activity level is just 3 Ci after 50 years. The graphite shells are supported on an aluminum alloy structure so that the entire blanket radioactivity drops substantially even after such a period as short as one week. Hence limited hands-on maintenance appears feasible which should greatly simplify blanket replacement. Assembly and disassembly procedures for this modular blanket design have been developed. The blanket segments can be readily removed by opening the sphere in quadrants after halting the $Li_2O$ flow. The estimated annual downtime for blanket segment replacement is two weeks. The biological hazard potential (BHP) defined as the radioactivity in $Ci/kW_t$ divided by the maximum permissible concentration in air ($MPC_a$) as established by U.S. Federal Guidelines is shown in Fig. 8. For comparison, a curve generated by Häfele et al.[13] for LMFBR fuel is also shown. The radioactivity levels in the case of SOLASE are $10^{-8}$ of the levels from LMFBR fuel after about one to two human generations (approximately 50 years).

Possible chemical reactions between the front wall of the blanket and materials from the pellet have been investigated. The reaction rates between the unburned hydrogen isotopes and the graphite front wall have been

estimated at the front wall temperature of interest ( 1800°C) and acetylene will be formed. For pellet designs of interest the erosion rate can be limited to about 2 mm/yr by rapid pumping. The corresponding pumping power required is less than 10 MW. Special attention has been given to possible non-hydrogenic pellet constituents and their separation from the reactor exhaust gases. Several pellet compositions containing glass, organic polymers, and high-Z materials have been considered. Xenon appears to be an ideal high-Z component although the use of lead or mercury in the pellet does not pose significant problems since they do not form stable carbides.

The volumetric heat generation decreases away from the first wall and the $Li_2O$ particle velocity distribution is tailored to accommodate this effect. Faster flow is provided near the front wall in order to remove the surface heat flux. The shaping of the velocity profile is accomplished by means of adjustable baffles at the exit of the six radial zones. The required velocities (see Fig. 7) are low so that structural erosion does not appear to be a problem. The aluminum alloy back structure on which the blanket is supported is water-cooled and is maintained at 150°C. The power removed at such a low temperature is small and is added to the steam cycle through a feed water heater.

The effect of radiation damage on the graphite structural segments has been analyzed. A lifetime estimate has been made based upon the criterion that the stresses in the blanket should not exceed 50% of the tensile strength of the material. A self-consistent inelastic structural analysis has been performed which follows the distribution of the stresses

during operation and after shutdown or restart as a function of time. It is found that both the radiation induced dimensional changes and the initial graphite porosity are critical to the prediction of changes in the elastic properties and therefore of the tensile strength.

The results of the analysis show that the structure must not be rigidly constrained at its boundaries in order to avoid excessive thermal and swelling stresses. The stresses generated internally by differential shrinkage and growth are sufficiently relieved during operation by irradiation creep. The life-limiting stresses appear to be those that would be generated by the reversal of thermal stresses upon reactor shutdown. The safe limit of the tensile strength is found to decrease with increasing graphite porosity. This can be another life-limiting factor.

A number of important conclusions can be drawn from these results. The graphite structure must either be manufactured as a high-density material (~5% initial porosity) or a tailored density distribution must be achieved so that the dense graphite is in the high-flux and medium temperature region (~1000°C). The mechanical connections between the blanket structure and its surrounding support structure must be flexible. These two basic requirements are well within the range of present-day technology. Nevertheless, the behavior of graphite under irradiation is based in this analysis on models which need further experimental verification, particularly with regard to irradiation at high temperatures (>1200°C) and high fluences (>10 dpa). Since the extrapolation of graphite behavior under irradiation is rather modest in this study, the results

indicate that graphite is a suitable structural material for the blanket of fusion reactors and that lifetimes of about one year or more are realistic.

The effects of irradiation on the $Li_2O$ particles are also important and one might expect radiation enhanced densification such as has been found in $UO_2$ fuel in light water fission reactors. However, our analysis shows that radiation-enhanced densification in $Li_2O$ will not occur because the stopping power of the recoiling atoms is too small to result in localized melting.

In summary, the blanket design used in SOLASE offers many advantages including low cost, low weight, low induced radioactivity levels, the potential for hands-on maintenance, modular construction, low pressure, adequate breeding, low tritium inventory and leakage, and sufficiently long life. It is particularly suitable for inertial confinement fusion reactors since the vacuum requirements are not stringent. It is superior to blankets with metallic first walls and protective liners inasmuch as the neutron wall loading in such designs is limited by the ability to radiate the ion and photon energy deposited in the liner to the cold first wall. Such designs may however be more suitable for magnetic confinement systems. While the $Li_2O$ particles act as a good heat transport medium to remove the heat generated within the blanket (high $\rho C_p$/circulating power), the heat transfer coefficient between the first wall and the particle stream is quite low. This makes it possible to operate the front wall at tempertures significantly different from those of the blanket coolant.[14] The latter are dictated by power cycle efficiency

requirements while the former can be selected on the basis of radiation damage considerations. For this graphite blanket, the front wall temperature is sufficiently high to avoid runaway swelling. On the other hand, for blankets with metallic first walls and protective liners, the first wall can be maintained at temperatures well below those of the $Li_2O$ stream without having an adverse effect on the overall thermal efficiency of the plant.[14] In such systems the first wall can be separately cooled and maintained at a temperature that maximizes the structure lifetime. Overall the use of lithium oxide as a coolant and breeder in fusion systems (both inertial and magnetic confinement) allows great flexibility in system design.

## V. Major Conclusions and Technological Implications

A number of major issues have emerged from this work. Some of these are related to the general laser and pellet performance assumptions while others have to do with certain specific design approaches taken in SOLASE itself. We summarize these issues here and include comments on topics we have studied but did not report upon in this paper.

1. An energy gain on target of 100 to 200 or higher is difficult to achieve with a 1 MJ laser and although high gain target designs have been reported[15] they still must be verified by experiment. The basic question is whether the laser energy can be coupled into the target efficiently enough to make the target work. Physics analysis performed as part of this study shows that inertial confinement systems will have much better energy economics (higher pellet gain and yield) if larger laser (or other driver) input energy can be used. We have also found that small deviations from the perfect pulse shape required to achieve isentropic compression can sharply reduce pellet performance. The experiments planned

in the next several years should bring us much closer to an answer on this matter. Clearly the next 1 to 5 years will be critical for physics developments in the field.

2. The assumption that a laser design with multipassing of the last two amplifiers can have an efficiency of about 7% must be verified. In particular a laser that has this efficiency and also has the appropriate wavelength and pulse shaping characteristics required. If very large gains are possible, e.g., $G = E_{TN}/E_L > 500$, then lower efficiency lasers can be considered. However if the incident laser energy remains at or more than 1 MJ, the implied large pellet yield will pose unique cavity design problems and low laser efficiency, even offset by high pellet gain, could prove uneconomical because of high power supply costs. (That is, while the recirculating power fraction is determined by $\eta_L G$, the laser costs depend on the absolute values of $\eta_L$ and $E_L$.)

There is at present no laser that clearly meets all the requirements for laser fusion. Several lasers can potentially have an efficiency exceeding 1%. Further, if the pulse width can be longer than 1 ns (e.g. 5-20 ns), then the design of a laser would become easier and in some cases the efficiency would improve.

3. The development of power supplies and very short pulsed switches (1 μs or so) that can operate reliably for $10^8$-$10^9$ shots are clearly critical.

4. The gas protection method analyzed for SOLASE using either neon or xenon at 0.1-1 torr pressure to prevent charged particle debris (and X-rays in the case of xenon) from reaching the first wall and last mirror requires verification. At the laser intensity level required ($>10^{15}$ W/cm$^2$) on target, gas breakdown will occur but this may not be serious

for reactor size targets with radii on the order of 2 mm. The applicability of this concept can be tested in both present and near term laser experimental facilities.

5. A key issue is the development of a basic manufacturing procedure for the mass production of targets at an acceptable investment of capital. The delivery of targets into the reactor chamber appears feasible but trajectory correction in flight will be very difficult. A major issue for reactors both near and long term will be the maintenance of proper alignment in the laser optical train and the possible tracking of targets.

6. The tritium inventory in such reactors may be dominated by the tritium associated with the filling and storage of targets. For SOLASE a one week inventory is employed to allow operation during a malfunction in any part of the tritium cycle external to the reactor. There is also an inventory associated with pellets being fabricated and with other reactor subsystems such as the vacuum pumps and the reactor blanket. However the inventory is dominated by the pellet inventory and particularly by the time to fill a target with DT fuel.

In general, cryogenic targets consist of multiple layers. Working out from the center of a sphere, these layers include a central void, the DT fuel, a capsule, a high Z tamper layer, and a low Z, low density ablative layer. The capsule layer may be glass or a polymer such as polyvinyl alcohol (PVA). The diffusion rates of DT through glass are much lower than the rates through PVA so that the estimated total plant tritium inventory is approximately 10 kg with PVA encapsulation and 25 kg with glass capsules.

There is therefore a strong incentive to use polymer encapsulation. This is incidentally just one of many examples where pellet design has a significant impact on reactor analysis.

7. The performance of graphite composite blanket segments under reactor irradiation must be verified, particularly at temperatures above 1200°C. The temperature decoupling of the graphite and $Li_2O$ offers the possibility of operating the graphite at optimal temperatures but the reversal of thermal stresses on reactor shutdown could limit the blanket lifetime. The concept is extremely attractive from other viewpoints (e.g., very low induced radioactivity) and therefore deserves serious study in the future.

8. The design and protection of the last mirror poses no insuperable difficulties unless dielectric coatings are required. Such coatings are essential for lasers in the optimum 3000-6000 Å range in order to obtain adequately high mirror reflectivity (> 99%). Yet neutron damage to such coatings through the formation of color centers can occur at very low fluence levels. Unless overcome, this problem may prohibit the use of visible lasers.

9. The vacuum requirements of laser fusion reactors may be modest if the pumping speed is set by wall erosion limits. However, the key issues relate to the nature of the pellet debris, the influence of materials remaining in the gas on laser beam transport and gas breakdown, and the energy content of the gas flowing from the chamber. Separation techniques are required to handle the radioactive chamber effluent, the unburnt tritium, and other materials that are recycled to the pellet factory. A defniitive answer on vacuum requirements must await the availability of the final target design for reactor applications.

10. The use of multiple cavities rather than a single cavity was briefly investigated. The primary motivation is to increase the potential availability time of the reactor. On the contrary, we have found that the most reliability-sensitive subsystem is the laser rather than the reactor chamber. Multiple lasers and power supplies, while not economically attractive, would be preferable to multiple cavities. Further the use of multiple cavities increases the complexity of the beam line system and decreases the attractive accessibility feature of laser fusion.

11. The success and choice of a cavity design will strongly depend on pellet materials and output characteristics. At this time little information is available on this subject. It is likely that a generic design not dependent on the pellet output spectra will not be optimum and will not make laser fusion appear as attractive as it ultimately might be.

12. An unprotected dry wall cavity design made from any reasonable material will not survive a microexplosion at "economically reasonable" wall loadings ($\gtrsim$ 1 MW/m$^2$) for the following reasons:

(a) Excessive Thermal Ablation: Both graphite and metallic first walls (Mo, Ta, SS) will experience large surface temperature excursions since the ions and soft X-rays deposit their energy in a thin surface layer. Excessive ablation (>1 cm/y) will take place.

(b) Sputtering: Sputtering will be significant (> 1 cm/y) since damage occurs at elevated temperatures. (Sputtering yields increase sharply as the surface approaches the melting temperature).

Spallation does not appear to be a problem since there will be no thermoelastic stress wave from ion energy deposition (because of the spread in arrival time). Also, if the X-ray spectrum is harder than about a 1 keV black body, only small amplitude transient stresses will be generated.

13. The blanket tritium inventory in SOLASE can be on the order of 1 kg but the exact method of tritium recovery will depend on the purity of the $Li_2O$, the value of the tritium diffusivity (presently unknown), and the porosity of the $Li_2O$ microspheres. Tritium release rates from the plant through the steam generators and reheaters appears to be acceptably low. This rate is 4-6 Ci/day or 40-60 nCi/l of water so that the $Li_2O$ blanket concept appears to be compatible with a power cycle that does not have an intermediate loop.

The tritium reprocessing system for the pellet debris is strongly dependent on both pellet and cavity design. Chemical reactivity with the cavity wall as well as the potential variety of materials that might be used in the target complicate the problem. While we have analyzed the issue for a pellet design in SOLASE, more information on pellet composition will be required before a firm assessment of the difficulties here can be made.

14. A general advantage of laser fusion reactors is that the reactor cavity and blanket are not surrounded by complex magnet systems. This greatly

improves access. However if uniform illumination of the target is required this advantage tends to be offset by a complex beam delivery system with mirrors that must be closer to the target.

## V. General Prognosis

The experiments outlined on Table 4 may produce substantial successes in the physics of pellet implosion over the next several years. If a gain on target of 100 is achieved, as predicted for the NOVA and Angara V facilities, then the physics basis for targets applicable to inertial confinement fusion reactors will have been demonstrated. At that point, the key technical issues will be those described in the previous section. Thus, the findings of studies such as SOLASE, when taken together with results of experiments carried out over the next 5-7 years with ever increasing energy and power on target, should establish whether an ambitious engineering-oriented program aimed at reactor development is warranted.

## References


1. G. Charatis, et al., in Plasma Physics and Controlled Nuclear Fusion Research 1974 (Proc. Int. Conf., Tokyo, 1974), IAEA, Vienna (1975), Vol. II, 317.

2. J. Holtzrichter, et al., in IEEE Second International Conference on Plasma Science, IEEE, Ann Arbor (1975), p. 85.

3. E. K. Storm, et al., "Laser Fusion Experiments at 2 TW", presented at the 10th Eur. Conf. on Laser Interactions With Matter, Talaiseau, France (Oct. 18-22, 1976).

4. D. Giovanelli, et al., "Laser Fusion Target Interaction Studies at 10.6 μm", in Proceedings of Conference on Laser Engineering and Applications, Washington, D.C. (June 1-3, 1977).

5. S. L. Bogolyubskij, et al., in Plasma Physics and Controlled Nuclear Fusion Research 1976 (Proc. Int. Conf., Berchtesgaden, 1976), IAEA, Vienna (1977), Vol. I, 1977.

6. J. Chang, et al., "Neutron Production From Advanced REB Fusion Targets", Sandia Laboratory Report, SAND-77-2017 (March 1977).

7. J. Nucholls, L. Wood, A. Thiessen, and G. Zimmerman, Nature 239, 139 (1972).

8. K. Brueckner and S. Jorna, Rev. Mod. Phys. 46, 325 (1974).

9. R. W. Conn, et al., "SOLASE, A Laser Fusion Reactor Study", Fusion Research Program Report, UWFDM-220 (University of Wisconsin, 1977).

10. G. A. Moses, Nucl. Sci. Eng. 64, 49 (1977). See also, G. A. Moses, "PHD-IV-A Plasma Hydrodynamics-Thermonuclear Burn-Radiative Transfer Computer Code", Fusion Research Program Report FDM-194, University of Wisconsin (February 1977).

11. J. Lindhard, M. Scharff, and H. E. Schrott, Mat. Fys. Medd. Dan. Vid. Selsk. 33, 14, (1963). See also, I. Manning and G. P. Muller, Comp. Phys. Comm. 6, (1973).

12. R. Spencer, University of Wisconsin (private communication). See also, S. Goldberg and M. Abarbanel, J. Comp. Phys. 10 ,1 (1972).

13. W. Häfele, et al., "Fusion and Fast Breeder Reactors", International Institute for Applied Systems Analysis Report, RR-77-8, IIASA, Laxenburg, Austria (July 1977).

References (cont.)

14. R. W. Conn, et al., "Studies of the Technological Problems of Laser Driven Fusion Reactors", Fusion Research Program Report, UWFDM-190 (University of Wisconsin, Jan. 1977).

15. J. Lindl, "High Gain Targets for Advanced Laser System", Bull. Amer. Phys. Soc. 22, 1078 (1977). Also, J. Lindl, "Low Aspect Ratio Double Shells for High Density and High Gain", Topical Meeting on Inertial Confinement Fusion (to be published, Optical Soc. of America, Feb. 1978).

## Figure Captions

FIG. 1 Top view of the SOLASE laser fusion reactor design. The laser building on the right has beam delay lines indicated as dashed lines.

FIG. 2 Cross section view of the reactor cavity. The chamber is filled to a density of about $10^{16}$ $cm^{-3}$ with a buffer gas. Ne or Xe are the most likely candidates. The suppression chamber is for pumping and to weaken any propagating shocks. Gas flows in front of the mirror to the chamber stopping residual charged particles and X-rays. Details of the blanket are seen at the upper right.

FIG. 3 The various power flows in the SOLASE reactor design. The recirculating power fraction is about 28%.

FIG. 4 Illustration of scheme for flowing a noble gas to protect the last optical element in the laser beam train.

FIG. 5 Cross section view of the final annular amplifier designed to give an output energy of 45.8 kJ. There are 6 such amplifiers through which four beams are sequentially passed with a separation of about 100 ps. The 24 resulting beams are then combined in pairs to produce the 12 final beams that illuminate the target.

FIG. 6 First wall temperature rise as a function of the X-ray spectrum and characterized by a black body temperature. Two different cavity fill gases, neon and xenon, at different fill pressures were used for comparison. The energy released in X-rays for the purpose of this graph is 15 MJ but $\Delta T$ varies linearly with the energy in X-rays for a given value of $\theta_{BB}$.

FIG. 7 Detailed schematic of the cavity blanket designed for SOLASE. Lithium oxide ($Li_2O$) particles of mean radius 100 $\mu$ flow under graphite through the blanket frame made from composite graphite. The $Li_2O$ flow velocity is tailored to produce a uniform exit temperature of 600°C. The graphite itself operates at a significantly different temperature from the $Li_2O$ and is useful in controlling radiation damage to the structure. The chamber is composed of 16 such segments.

FIG. 8 The decay of the biological hazard potential as a function of time after shutdown for the SOLASE blanket with various backing materials (see Fig. 3). The BHP is the activity in $Ci/kW_{th}$ divided by the maximum permissible concentration (MPC). The curve for the LMFBR from Häfele et al.[10] includes reprocessing the fuel after one year.

TOP VIEW OF SOLASE

A CONCEPTUAL LASER FUSION REACTOR POWER PLANT

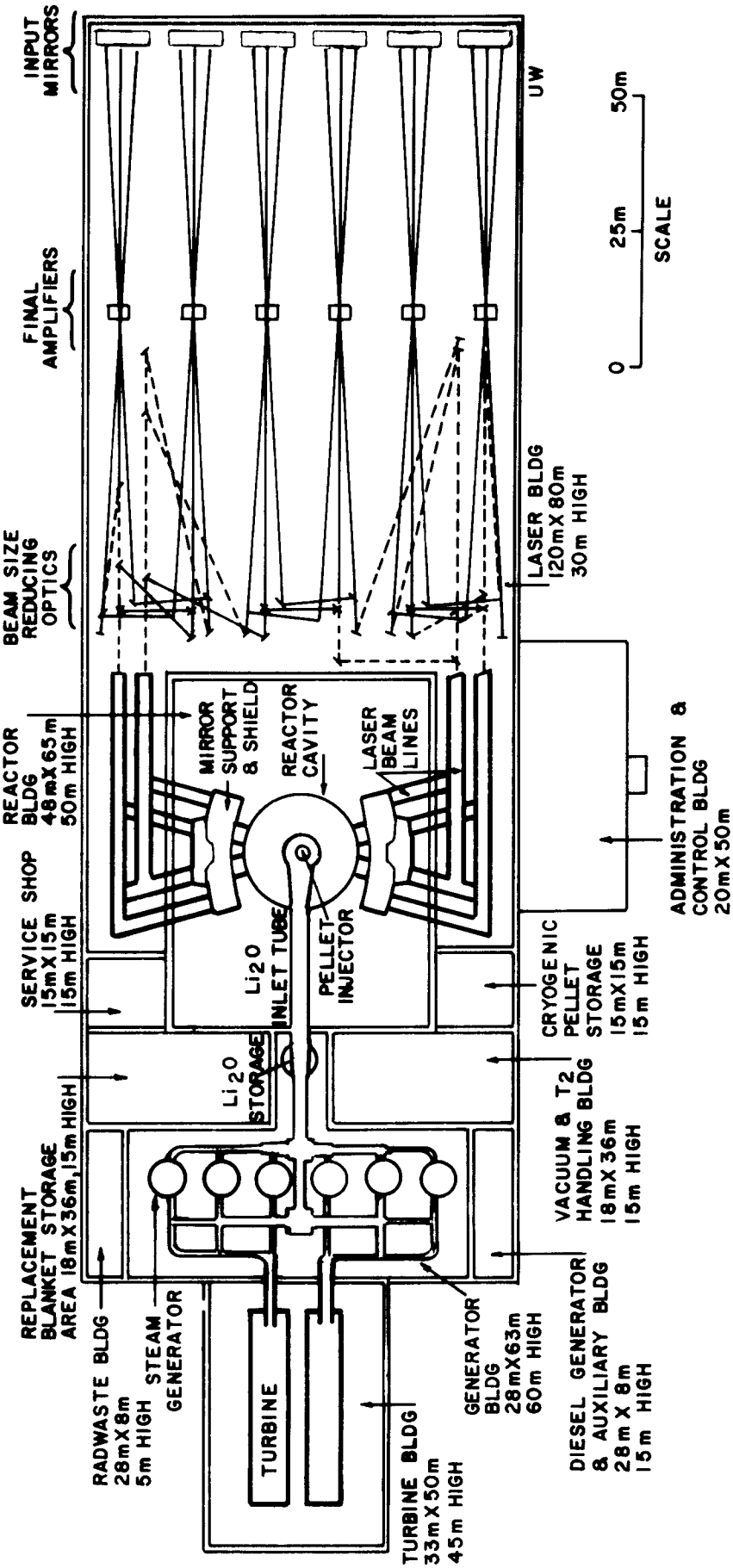


FIG. 1

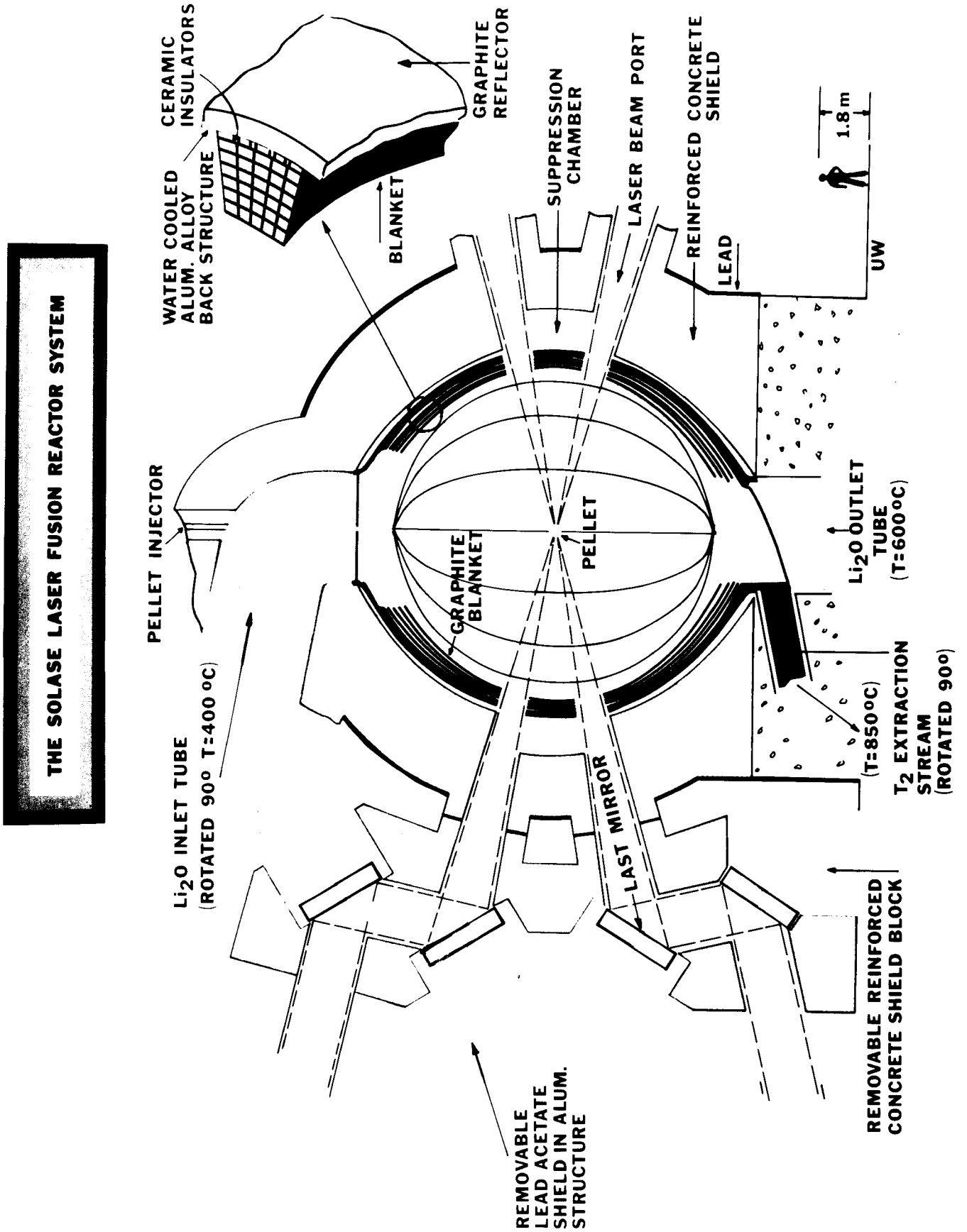
THE SOLASE LASER FUSION REACTOR SYSTEM
CERAMIC INSULATORS
GRAPHITE REFLECTOR
WATER COOLED ALUM. ALLOY BACK STRUCTURE
BLANKET
SUPPRESSION CHAMBER
LASER BEAM PORT
REINFORCED CONCRETE SHIELD
LEAD
1.8 m
UW
PELLET INJECTOR
GRAPHITE BLANKET
PELLET
$Li_2O$ OUTLET TUBE (T=600°C)
$Li_2O$ INLET TUBE (ROTATED 90° T=400 °C)
(T=850°C)
$T_2$ EXTRACTION STREAM (ROTATED 90°)
LAST MIRROR
REMOVABLE REINFORCED CONCRETE SHIELD BLOCK
REMOVABLE LEAD ACETATE SHIELD IN ALUM. STRUCTURE

FIG. 2

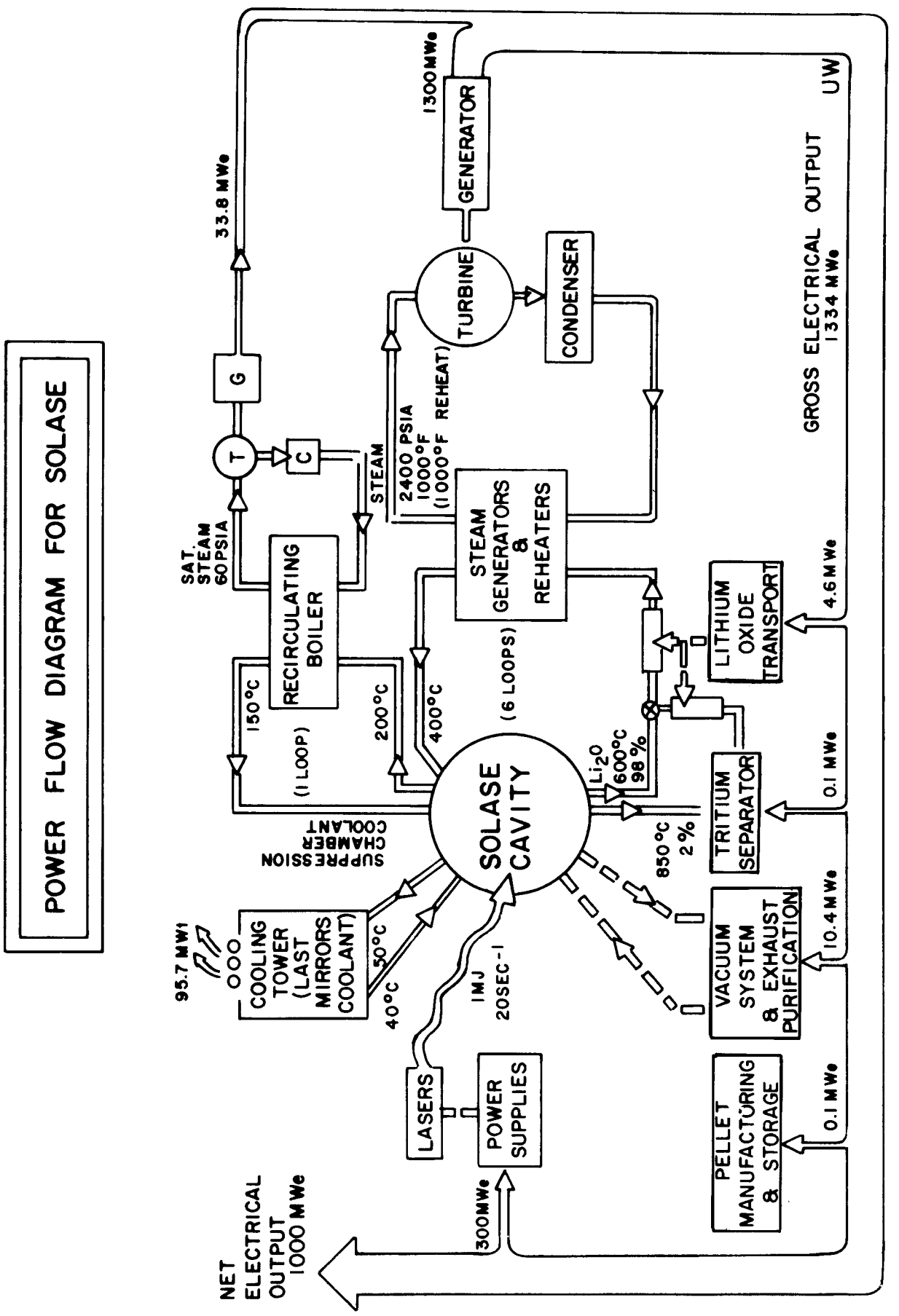
POWER FLOW DIAGRAM FOR SOLASE
NET ELECTRICAL OUTPUT 1000 MWe
300MWe
33.8 MWe
1300MWe
GENERATOR
GROSS ELECTRICAL OUTPUT 1334 MWe
UW
TURBINE
CONDENSER
G
T
C
STEAM
2400 PSIA
1000°F
(1000°F REHEAT)
SAT. STEAM 60PSIA
RECIRCULATING BOILER
STEAM GENERATORS & REHEATERS
(6 LOOPS)
(1 LOOP)
150°C
200°C
400°C
SUPPRESSION CHAMBER COOLANT
SOLASE CAVITY
$Li_2O$ 600°C 98 %
850°C 2 %
LITHIUM OXIDE TRANSPORT
4.6 MWe
TRITIUM SEPARATOR
0.1 MWe
95.7 MWt
COOLING TOWER (LAST MIRRORS COOLANT)
40°C
50°C
IMJ 20SEC-1
LASERS
POWER SUPPLIES
VACUUM SYSTEM & EXHAUST PURIFICATION
10.4 MWe
PELLET MANUFACTURING & STORAGE
0.1 MWe

FIG. 3

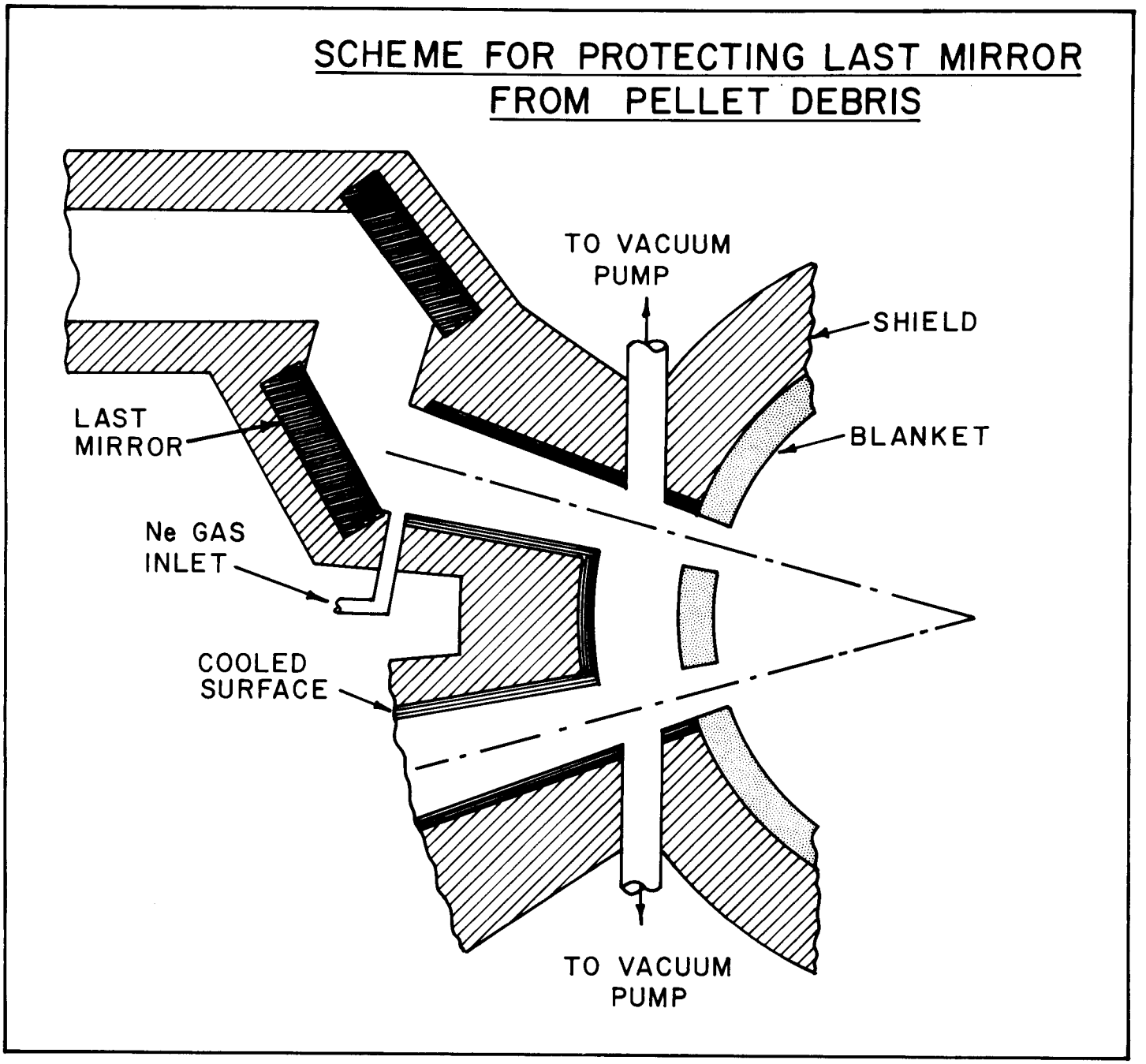
SCHEME FOR PROTECTING LAST MIRROR FROM PELLET DEBRIS
TO VACUUM PUMP
SHIELD
LAST MIRROR
BLANKET
Ne GAS INLET
COOLED SURFACE
TO VACUUM PUMP

FIG. 4

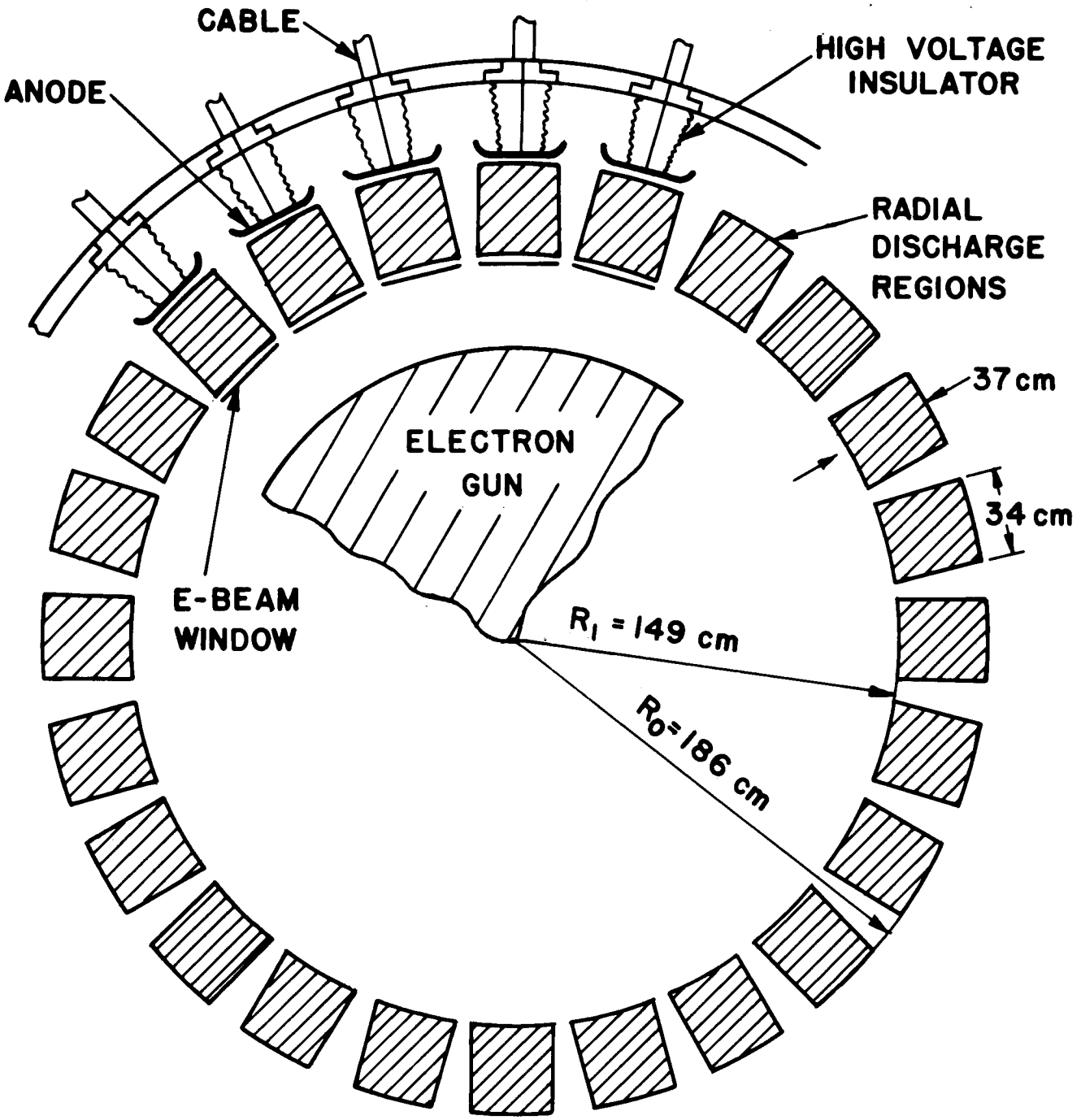


END VIEW OF ANNULAR AMPLIFIER FOR SOLASE

FIG. 5

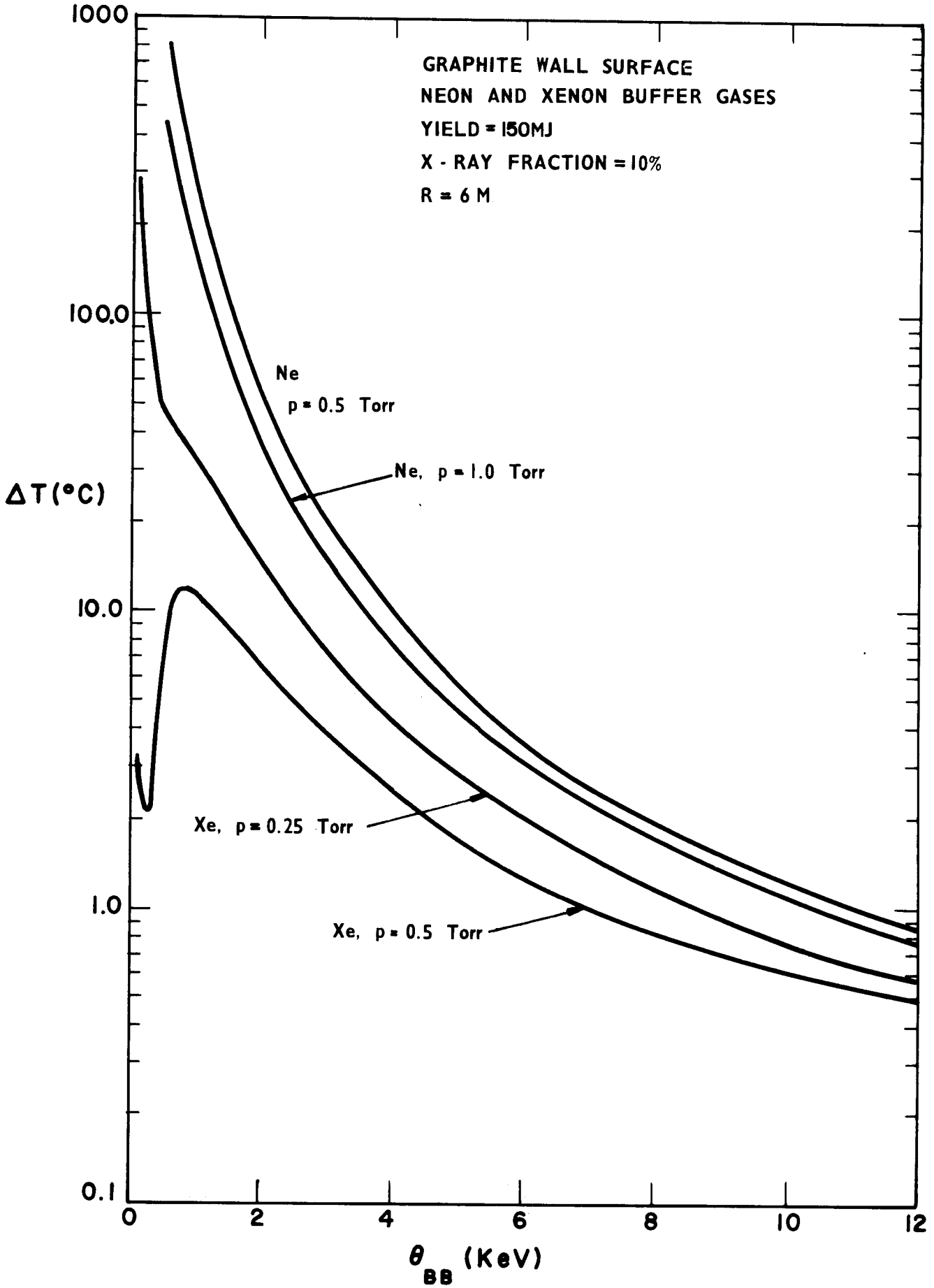
GRAPHITE WALL SURFACE
NEON AND XENON BUFFER GASES
YIELD = 150MJ
X - RAY FRACTION = 10%
R = 6 M
Ne
p = 0.5 Torr
Ne, p = 1.0 Torr
Xe, p = 0.25 Torr
Xe, p = 0.5 Torr
ΔT(°C)
1000
100.0
10.0
1.0
0.1
0
2
4
6
8
10
12
θBB (KeV)

FIG. 6

# SCHEMATIC OF GRAPHITE BLANKET SEGMENT FOR SOLASE

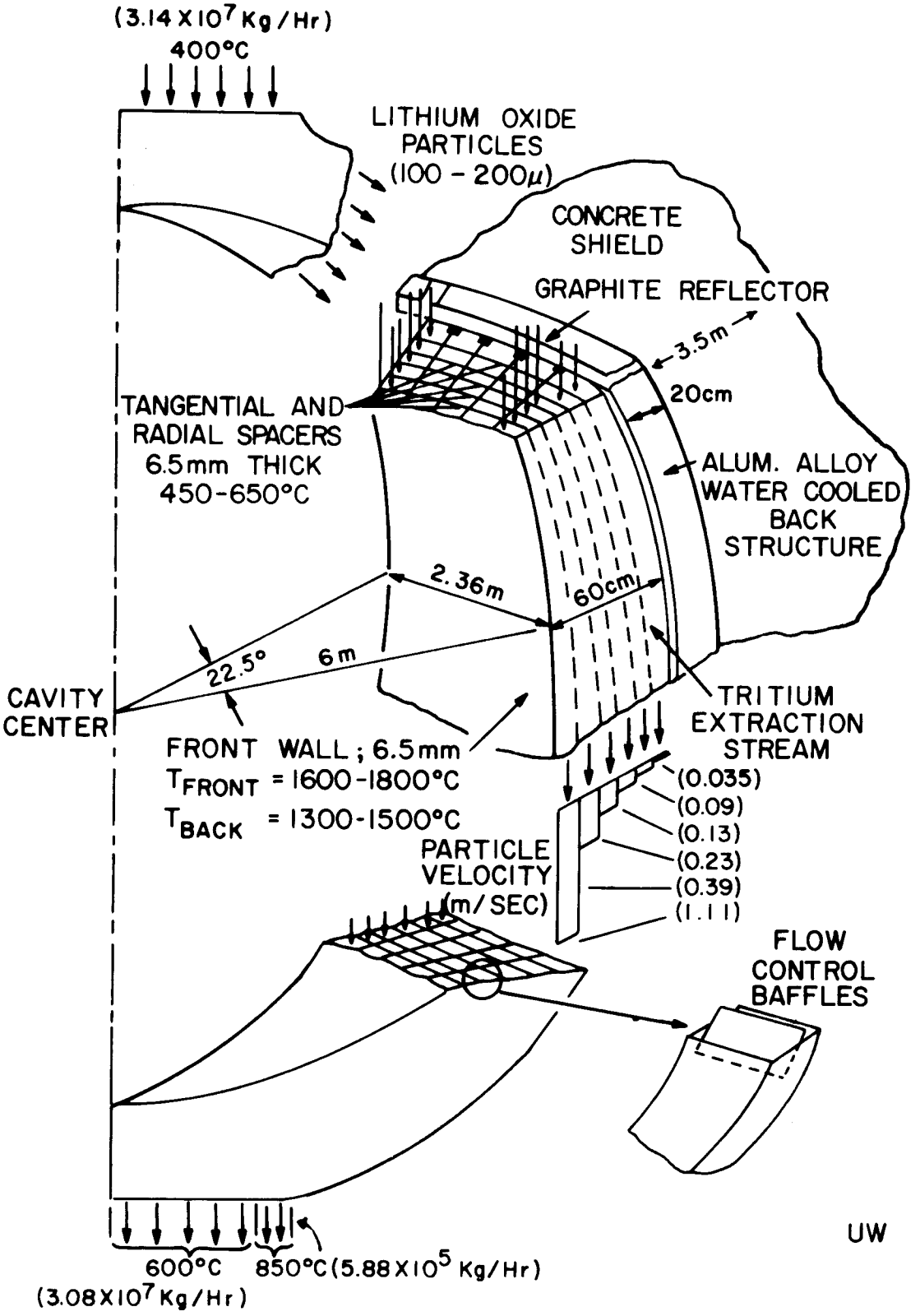


FIG. 7

# BIOLOGICAL HAZARD POTENTIAL IN AIR FOR LASER FUSION BLANKET – ONE YEAR OPERATION

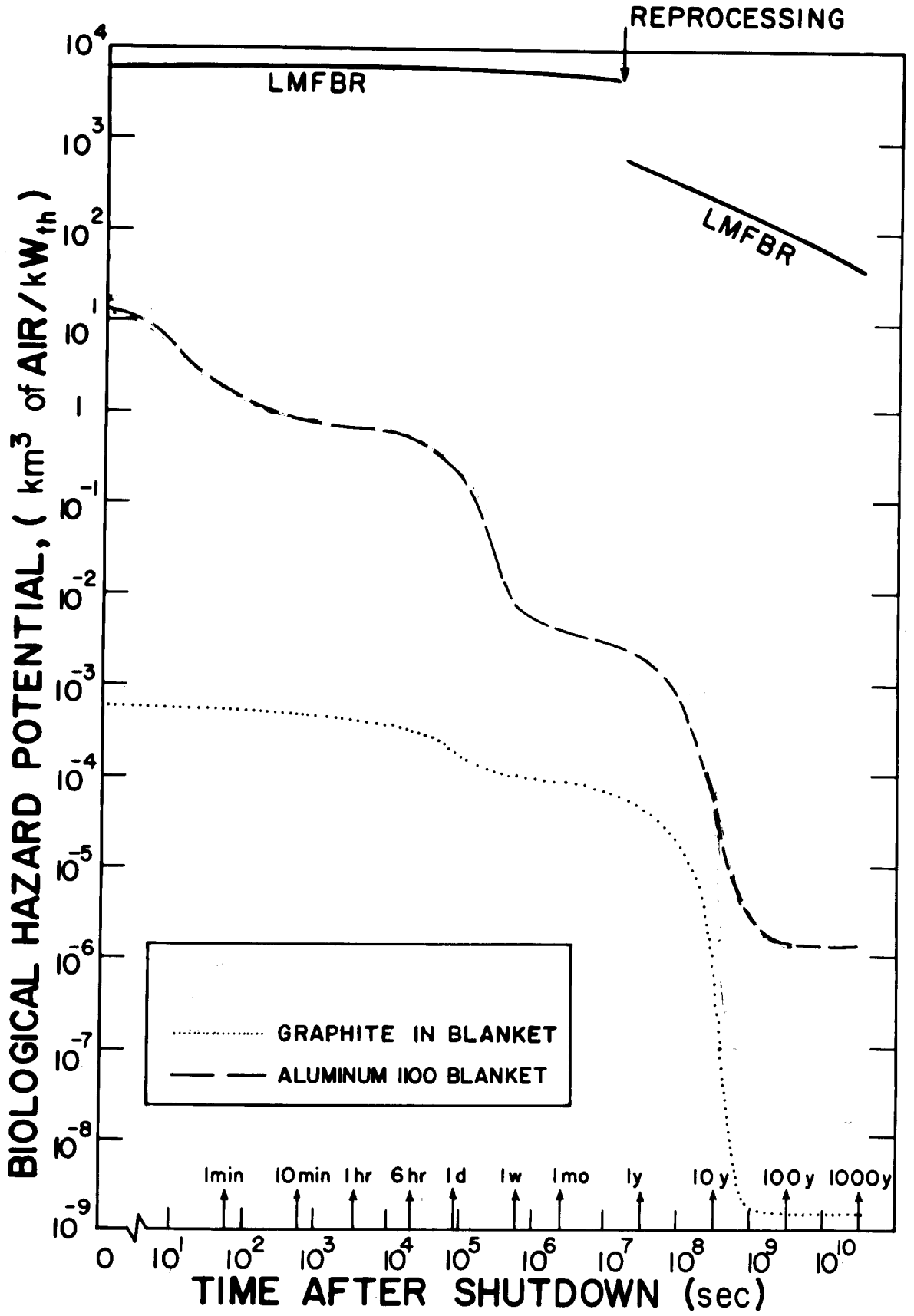


FIG. 8

Table 1

Parameters for the SOLASE Laser Fusion Reactor

| | |
|---|---|
| CAVITY SHAPE | SPHERICAL |
| CAVITY RADIUS | 6 m |
| 14 MeV NEUTRON WALL LOADING | 5 $MW/m^2$ |
| THERMAL POWER | 3340 MW |
| GROSS ELECTRICAL POWER | 1334 MW |
| NET ELECTRICAL POWER | 1000 MW |
| RECIRCULATING POWER FRACTION | 28% |
| NET PLANT THERMAL EFFICIENCY | 30% |
| LASER TYPE | GAS PHASE |
| LASER ENERGY ON TARGET | 1 MJ |
| LASER EFFICIENCY (WITH MULTIPASSING) | 6.7% |
| NUMBER OF FINAL AMPLIFIERS | 6 |
| NUMBER OF FINAL BEAMS | 12 |
| ENERGY OUTPUT/AMPLIFIER PASS | 45.8 kJ |
| PULSE WIDTH | 1 ns |
| PULSE REPETITION RATE | 20 Hz |
| PELLET YIELD AND GAIN | 150 MJ |
| FRACTIONAL BURNUP OF FUEL | 45% |
| INITIAL FUEL MASS | 1 mg |
| GENERIC TARGET DESIGN | MULTILAYERED-CRYOGENIC |

Table 2

Parameters for the SOLASE Laser Fusion Reactor

| | |
|---|---|
| TARGET ILLUMINATION | TWO SIDED |
| NUMBER OF FINAL MIRRORS | 12 |
| F/No. of FINAL MIRROR | 7.5 |
| DISTANCE FROM LAST MIRROR TO PELLET | 15 m |
| DIAMETER OF LAST MIRROR | 3.5 m |
| COMPOSITION OF LAST MIRROR | Cu on Al |
| MANUFACTURING PROCEDURE | DIAMOND TURNING |
| FIRST WALL PROTECTION METHOD | Ne or Xe BUFFER GAS |
| BLANKET STRUCTURE | GRAPHITE COMPOSITE |
| BLANKET BREEDING AND HEAT TRANSPORT MEDIUM | LITHIUM OXIDE ($Li_2O$) |
| TRITIUM BREEDING RATIO | 1.33 |
| TOTAL ENERGY PER FUSION EVENT | 18.6 MeV |
| TOTAL $Li_2O$ FLOW RATE | $3.12 \times 10^7$ kg/hr |
| AVERAGE $Li_2O$ FLOW VELOCITY | 0.7 m/s |
| $Li_2O$ INLET TEMPERATURE | $400^oC$ |
| $Li_2O$ OUTLET TEMPERATURE | $600^oC$ |
| TRITIUM INVENTORY | |
| GLASS ENCAPSULATION OF TARGET | 24.7 kg |
| POLYMER ENCAPSULATION OF TARGET | 10.9 kg |
| TOTAL REACTOR RADIOACTIVITY LEVEL 50 YEARS AFTER SHUTDOWN | 3 Ci |

Table 3

Ranges in Neon ($1.5 \times 10^{16}$ $cm^{-3}$) For Different Particles Found in the Pellet
(The Energies Given Are The Maximum Values For Each Particle)

| Particle | Energy | Mean Range (m) | RMS Deviation |
|---|---|---|---|
| D | 20 keV | 2.3 | 0.1 |
| T | 30 keV | 3.4 | 0.2 |
| $^4He$ | 90 keV | 3.6 | 0.2 |
| Hg | 4.2 MeV | 4.9 | 0.8 |

Table 4

Near Term Experimental Drivers For
Inertial Confinement Fusion Experiments

| Laboratory | Driver | Power, TW | Completion Date | Anticipated Experimental Results |
|---|---|---|---|---|
| SANDIA-A | e-BEAM (PROTO-II) | 7 | 1977 | $10^7$ - $10^9$ NEUTRONS |
| LLL | Nd: GLASS LASER (SHIVA) | 10-40 | 1977 | ~ $10^{13}$ NEUTRONS |
| LASL | 8-BEAM $CO_2$ LASER | 10-20 | 1978 | $10^{10}$ - $10^{12}$ NEUTRONS |
| LLE-UR | Nd: GLASS LASER (OMEGA-10) | 3-30 | 1979-80 | USED FACILITY |
| SANDIA-A | e-BEAM (EBFA-I) | 30 (1 MJ, 40 ns) | 1980 | $10^{10}$ - $10^{13}$ NEUTRONS |
| KURCHATOV | e-BEAM (ANGARA-V) | 80 (5 MJ, 85 ns) | 1982 | G ~ 100 |
| LLL | Nd: GLASS LASER (NOVA) | 100-300 | 1983 | $10^{16}$ - $10^{19}$ NEUTRONS<br>G ~ 1 - 100 |
| LASL | $CO_2$ LASER (ANTARES) | 100-200 | 1982 | $10^{16}$ - $10^{17}$ NEUTRONS<br>G ~ 1 - 10 |
| SANDIA-A | e-BEAM (EBFA-II) | 60-80 | 1983-85 | $10^{15}$ - $10^{17}$ NEUTRONS<br>G ~ 0.1 - 10 |